Journal of Magnetism and Magnetic Materials 592 (2024) 171781

Contents lists available at ScienceDirect

Journal of Magnetism and Magnetic Materials

journal homepage: www.elsevier.com/locate/jmmm

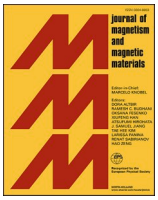

Separating the contributions of the magnetic subsystems in antiferromagnetic ferrihydrite nanoparticles by analyzing the magnetization in fields of up to 250 kOe

A.A. Krasikov [a], D.A. Balaev [a,*], A.D. Balaev [a], S.V. Stolyar [a,b], R.N. Yaroslavtsev [a,b], R.S. Iskhakov [a]

[a] Kirensky Institute of Physics, Federal Research Center of Siberian Branch of Russian Academy of Sciences, Krasnoyarsk, Russia
[b] Federal Research Center of Siberian Branch of Russian Academy of Sciences Krasnoyarsk, Russia

A B S T R A C T

Contributions of different magnetic subsystems formed in the systems of synthetic ferrihydrite nanoparticles (characterized previously) with an average size of $< d > \approx 2.7$ nm coated with polysaccharide arabinogalactan in different degrees have been separated by measuring the dependences of their magnetization M on magnetic field H of up to 250 kOe on vibrating sample and pulsed magnetometers. The use of a wide measuring magnetic field range has been dictated by the ambiguity in identifying a linear $M(H)$ portion for such antiferromagnetic nanoparticle systems within the conventional field range of 60–90 kOe. The thorough analysis of the magnetization curves in the temperature range of 100–250 K has allowed the verification of the contributions of (i) uncompensated magnetic moments μ_{un} in the superparamagnetic subsystem, (ii) the subsystem of surface spins with the paramagnetic behavior, and (iii) the antiferromagnetic susceptibility of the antiferromagnetically ordered ferrihydrite particle core. As a result, a model of the magnetic state of ferrihydrite nanoparticles has been proposed and the numbers of spins corresponding to magnetic subsystems (i)–(iii) have been estimated. An average magnetic moment μ_{un} of $\sim 145\,\mu_B$ (μ_B is the Bohr magneton) per particle corresponds approximately to 30 decompensated spins of iron atoms in a particle (about 3 % of all iron atoms), which, according to the Néel's hypothesis $\mu_{un} \sim < d >^{3/2}$, are localized both on the surface and in the bulk of an antiferromagnetically ordered particle. The fraction of free (paramagnetic) spins is minimal in the sample without arabinogalactan coating of the nanoparticle surface (7 %) and is attained 20 % of all iron atoms in the sample with the highest degree of spatial separation of particles. According to this estimation, paramagnetic spins are located mainly on the edges and protruding areas of particles. Most magnetic moments of iron atoms are ordered antiferromagnetically and the corresponding magnetic susceptibility of this subsystem behaves as in an antiferromagnet with the randomly distributed crystallographic axes, i.e., increases with temperature.

1. Introduction

A fundamental problem of the change in the magnetic properties of magnetically ordered substances with decreasing particle sizes has been studied for quite a long time [1–8]. The seemingly most striking and earliest discovered manifestation of this change was the transition from the multi-domain to single-domain magnetic state with a decrease in the size of ferro- and ferrimagnetic particles. The next most significant effect emerging with a decrease in the particle size is apparently the so-called superparamagnetic (SPM) limit, i.e., the particle size at which, at a certain temperature, thermal fluctuations prevail over the magnetic anisotropy energy. The aforesaid can be considered to be size effects, although these effects have other manifestations, for example, the modification of the relevant magnon dispersion law due to the finite boundary conditions and, as a consequence, the modification of Bloch's law [9,10]. To date, the critical sizes corresponding to these states have been determined for many magnetically ordered substances and the size-related features of changes in the magnetic properties of nanoparticle systems have been found [11–16].

In addition to the size effects, the effects related to the developed surface can also be distinguished. They manifest themselves most brightly when a number of atoms belonging to the particle surface is comparable with a number of atoms inside a particle. Here, concerning the magnetic properties, it should be mentioned that an additional contribution to the magnetic anisotropy energy, specifically, the surface magnetic anisotropy, arises, which is inversely proportional to the particle size [17–25]. Magnetically active atoms of the surface already have a local environment that differs from that of atoms in the bulk; therefore, an additional magnetic subsystem can form on the surface, which will affect the magnetic properties.

To succeed in the creation of new magnetic nanomaterials with desired properties for various applications, it is important to understand the above-mentioned surface and size effects. Therefore, it is urgent to establish the mechanisms responsible for imparting new (magnetic)

* Corresponding author.

https://doi.org/10.1016/j.jmmm.2024.171781
Received 27 December 2023; Received in revised form 22 January 2024; Accepted 23 January 2024
Available online 29 January 2024

properties with decreasing particle sizes by studying the surface and size effects of various magnetically ordered substances. The discussed effects can lead to the formation of magnetic subsystems, in addition to the initial one, in a chemically homogeneous nanoparticle. Here, an issue of the correct identification of new magnetic subsystems arises.

Object of this study ferrihydrite is a hydrated ferric oxide with the nominal formula $5Fe_2O_3{\cdot}9H_2O$, which only exists on the nanoscale (the maximal particle size is no more than 10 nm). The magnetic moments of iron atoms in ferrihydrite are ordered antiferromagnetically [26]. It would seem that the magnetic ordering of this type causes a very weak response to an external magnetic field. However, as was shown by Néel [5], structural defects in a fine antiferromagnetic (AFM) particle can lead to the new property: the uncompensated magnetic moment μ_{un}. The Néel's hypothesis was confirmed in quite a few studies on various AFM nanoparticle systems [20,26–53]. Among such systems, CuO [27], NiO [20,28–34], Cr_2O_3 [54], and β-FeOOH [55,56] can also be mentioned. According to the data reported in several studies, the magnetic moment μ_{un} per particle can attain hundreds of Bohr magnetons.

The classical consideration of the relationship between the thermal energy and magnetic anisotropy energy, which leads to the well-known Néel–Brown equation for the SPM blocking temperature, is also valid for AFM nanoparticles. Any magnetically ordered material is characterized by the magnetic anisotropy constant and, if the thermal energy significantly exceeds the magnetic anisotropy energy of the AFM particle, the antiferromagnetism vector in the AFM nanocrystal randomly changes its direction. Simultaneously, the uncompensated magnetic moment of the AFM nanoparticle exhibits the same SPM behavior. As the temperature decreases, both the antiferromagnetism vector and μ_{un} are blocked. The described behavior of AFM nanoparticles is consistent with the properties of ferro- and ferrimagnetic nanoparticles.

It is noteworthy that ferrihydrite is a component of ferritin, a complex that serves as an iron donor for living organisms and is, in fact, ferrihydrite in a protein shell. The magnetic properties of ferritin were discussed in numerous works (see, for example, [47–53]). Thus, ferrihydrite (and ferritin) can be attributed to the class of magnetic nanoparticles with the high application potential. The nontoxicity of ferrihydrite and, moreover, its antibacterial properties [44] make its nanoparticles promising for biomedicine [57–59]. As for the mechanisms of formation of the magnetic properties in ferrihydrite systems, they still remain not well understood, despite a great number of relevant works. Sometimes, different authors report the μ_{un} values differing by almost an order of magnitude for the systems with identical parameters of the particle size distribution. Moreover, different approaches to the interpretation of the experimental $M(H)$ curves were proposed [47,48,50,39–42,60–63].

The $M(H)$ dependence for a system of AFM nanoparticles in the SPM state is conventionally described by two or more components [50,64]. The first component is the Langevin function, which determines the SPM behavior of the moments μ_{un} with allowance for the $f(\mu_{un})$ distribution function related to the particle size. The second component is the field-linear contribution determined by the canting of ferromagnetically ordered sublattices of AFM particles (the AFM susceptibility) and other possible contributions. In most studies on ferrihydrite, it was observed that the AFM susceptibility decreases with temperature, which is atypical of an antiferromagnet with the random distribution of the crystallographic axes. A problem of interpreting the $M(H)$ dependences is that, in the conventional external field range of 50–90 kOe, the Langevin function does not saturate yet and the linear $M(H)$ portion might be determined incorrectly. In this work, it is proposed to interpret the magnetization curves using a wider external field range, in which this field-linear contribution could be correctly identified and the experimental $M(H)$ dependences could be interpreted. This will make it possible to determine the contributions of different magnetic subsystems formed in ferrihydrite nanoparticles. A similar approach was used in [31–33], where the $M(H)$ dependences for the systems of NiO nanoparticles were studied in pulsed fields of up to 250 kOe.

The aim of this study was to determine the contributions corresponding to the uncompensated magnetic moments, surface spins, and the AFM subsystem (the AFM particle core) by analyzing the magnetization curves of the ferrihydrite nanoparticle systems in fields of up to 250 kOe. For the sake of clarity, we limit the consideration to the temperature range of the SPM state of the particle magnetic moments, in which the irreversible behavior of the magnetization is not observed. An additional problem was to identify possible differences between the contributions of the magnetic subsystems in a series of samples in which ferrihydrite particles have identical sizes, but different degrees of spatial separation. In this regard, a series of samples of ferrihydrite nanoparticles coated with polysaccharide arabinogalactan (AG) in different degrees was examined. In this sample series, the intensity of the magnetic interactions between ferrihydrite particles decreases with an increase in the degree of particle coating (in the amount of AG) [65].

2. Experimental

2.1. Preparation and characterization of the samples

The technique for obtaining the synthetic ferrihydrite samples added with AG in different degrees was described in detail in [65]. At a certain stage of the ferrihydrite synthesis, AG in different relative concentrations was added. The three investigated samples were initial ferrihydrite without AG (sample FH-0) and ferrihydrite with two AG concentrations (samples FH-2 and FH-3, where the numbers correspond to the relative degrees of AG coating). The synthesis guideline suggested the identical sizes of individual ferrihydrite nanoparticles in the initial (FH-0) and coated (FH-2, FH-3) samples.

According to the transmission electron microscopy (TEM) data, the average particle size $< d >$ in ferrihydrite without an organic coating was 2.7 nm, which agrees well with the estimate obtained from the half-width of the first (brightest) diffraction ring in the microdiffraction pattern using the Scherrer formula [65–67].

The changes observed in the X-ray photoelectron spectra of Fe 2p, O 1 s, and C 1 s for the samples in the series FH-0, FH-2, and FH-3 are indicative of the formation of an organic coating of ferrihydrite nanoparticles, the thickness of which partially increases with the amount of added AG; in this case, no significant changes in the state of particles were detected [65].

The identity of ferrihydrite particles in all the three samples was also revealed by the analysis of Mössbauer spectra, which had the same parameters corresponding to the three nonequivalent iron positions typical of ferrihydrite (with a quadrupole splitting characteristic of each position) for all the samples [65].

2.2. Measurements of the magnetic properties

The $M(H)$ curves were measured in pulsed magnetic fields on an original setup at the Kirensky Institute of Physics, Siberian Branch of the Russian Academy of Sciences (Krasnoyarsk) [68] using the discharge of a capacitor battery through a solenoid. The investigated sample was securely fixed in an induction sensor of a pulse magnetometer. The pulse length was 16 ms. The magnetization was measured using an induction sensor, which is a system of compensated coils where the sample was placed. The signal induced in the coils was recorded by a digital storage oscilloscope. The $M(H)$ isotherms were obtained in the temperature range of 100–250 K at a magnetic field pulse amplitude of up to 250 kOe.

The data obtained with the pulse magnetometer were compared with the data of the quasi-static magnetic measurements carried out on a vibrating sample magnetometer [69] in fields of up to 60 kOe. The $M(H)$ dependences presented in this work contain the data of both the pulse magnetometer (0–250 kOe) and vibrating sample magnetometer.

3. Results and discussion

3.1. Processing of the M(H) dependences and the fitting parameters obtained

The temperature dependences of the magnetization for samples FH-0, FH-2, and FH-3 measured in weak external fields reveal distinct maxima at temperatures of 49, 22.3, and 18.3 K, respectively, upon zero-field cooling [65]. At low temperatures, the magnetization behavior is irreversible (there are the $M(H)$ hysteresis and the effect of the thermomagnetic prehistory on the $M(H)$ dependence); in the vicinity of the indicated temperatures, the irreversible behavior vanishes. The described behavior is unambiguously related to the transition of the uncompensated particle moments from the SPM state (at high temperatures) to the blocked state (at low temperatures). A decrease in the SPM blocking temperature in the sample series FH-0, FH-2, and FH-3 is consistent with the growing degree of arabinogalactan coating of ferrihydrite particles and is caused by weakening of the effect of the magnetic interparticle interactions on the SPM blocking processes [65,67].

Fig. 1 shows the $M(H)$ dependences for the samples under study at T = 100, 150, 200, and 250 K (symbols). The general view of these dependences is typical of AFM nanoparticle systems: in weak and moderate fields, the magnetization increases quite rapidly and, then, the $M(H)$ dependence gradually reaches a field-linear portion. The linear course of the magnetization curves begins in fields above 100 kOe. In the first approximation, the $M(H)$ dependence for a system of AFM particles with the same uncompensated magnetic moment μ_{un} (in the SPM state) can be written as

$$M(H) = M_0 \cdot L(\mu_{un}, H) + \chi_{total} \cdot H \quad (1)$$

where $L(\mu_{un}, H) = \coth(\mu_{un} \cdot H/kT) - 1/(\mu_{un} H/kT)$ is the Langevin function describing the alignment of particle magnetic moments μ_{un} in the applied magnetic field direction and M_0 is the saturation magnetization of the particle magnetic moment subsystem related to μ_{un} via number N_P of particles per unit sample mass (or volume): $M_0 = \mu_{un} \cdot N_P$. The temperature-dependent quantity χ_{total} determines the slope of the $M(H)$ curve in strong fields; this quantity was often identified with the magnetic susceptibility of an antiferromagnet [35–48]. Eq. (1) was used in [35–38,47] to describe the $M(H)$ dependences of AFM particles. Taking into account the distribution of the particle magnetic moments in the μ_{un} value, one can rewrite Eq. (1) as [50]

$$M(H) = M_{SPM}(H) + \chi_{total} \cdot H, \quad (2)$$

where the SPM behavior of the magnetic moments corresponds to the $M_{SPM}(H)$ function:

$$M_{SPM}(H) = N_P \int_0^\infty L(\mu_{un}, H) f(\mu_{un}) \mu_{un} d\mu_{un} \quad (3)$$

Here, $f(\mu_{un})$ is the magnetic moment distribution function (its relation to the size distribution is shown below). Usually, the log-normal distribution

$$f(\mu_{un}) = \left(\mu_{un} \cdot s \cdot (2\pi)^{1/2}\right)^{-1} exp\left\{ - [ln(\mu_{un}/n)]^2 / 2s^2 \right\}, \quad (4)$$

is used as $f(\mu_{un})$, in which the average particle magnetic moment is $<\mu_{un}> = n \cdot \exp(s^2)$ and s^2 is the $\ln(\mu_{un})$ dispersion. In both approaches (Eqs. (1) and (2)), there are several fitting parameters, but it is logical that only the $<\mu_{un}>$ value (μ_{un} in Eq. (1)) and the χ_{total} value can change with temperature.

The synthesis method used suggests the identical particle size distributions in samples FH-0, FH-2, and FH-3. In the samples with AG, the exact ferrihydrite content is unknown; some reasonable estimates were made in [65]. If particles of all the samples are in the same magnetic state, then their $M_{FH\text{-}0}(H)$, $M_{FH\text{-}2}(H)$, and $M_{FH\text{-}3}(H)$ dependences obtained at the same temperatures should coincide when divided by the coefficients corresponding to the ferrihydrite mass concentration x in the sample ($x = m_{FHYD}/(m_{FHYD} + m_{AG})$, where FHYD is ferrihydrite): $M_{FH\text{-}0}(H)/x_{FH\text{-}0} = M_{FH\text{-}2}(H)/x_{FH\text{-}2} = M_{FH\text{-}3}(H)/x_{FH\text{-}3}$. Here, $x_{FH\text{-}0} = 1$ and $x_{FH\text{-}3} < x_{FH\text{-}2}$; in this case, according to the data reported in [62], $x_{FH\text{-}3}$ and $x_{FH\text{-}2}$ can lie within 0.4–0.75. However, the experimental data from Fig. 1 cannot be scaled by this method.

At the next stage of processing of the experimental magnetization curves using Eq. (2), the fitting parameters were sought at which, along with the agreement between the experimental and calculated $M(H)$ dependences, the $f(\mu_{un})$ distribution function (Eq. (4)) would be identical for all the three samples (at the same temperatures). In this case, the N_P value can change from one sample to another, according to the relationship $N_{P\_FH\text{-}1} = N_{P\_FH\text{-}2}/x_{FH\text{-}2} = N_{P\_FH\text{-}3}/x_{FH\text{-}3}$ and the χ_{total} value can change as well. These parameters were found; the ferrihydrite concentrations in samples FH-2 and FH-3 were $x_{FH\text{-}2} \approx 0.56$ and $x_{FH\text{-}3} \approx 0.45$, which is consistent with the data from [65]. The Langevin terms in Eq. (2), i.e., the $M_{SPM}(H)$ dependences are shown in Fig. 1. They differ from one sample to another only by the determined coefficients $x_{FH\text{-}2}$ and $x_{FH\text{-}3}$.

The values obtained by fitting the χ_{total} value normalized to the ferrihydrite mass in the sample (χ_{total}/x) are presented in Fig. 2a. It can be seen that the $\chi_{total}(T)/x$ dependences decrease with the increasing temperature, as in the studies cited above. If we identify $\chi_{total}(T)$ with the AFM susceptibility of an antiferromagnet, the result obtained is atypical of an antiferromagnet with the random distribution of the crystallographic axes. In the latter case, the AFM susceptibility (hereinafter, $\chi_{AFM}(T)$) increases from low temperatures to the Néel

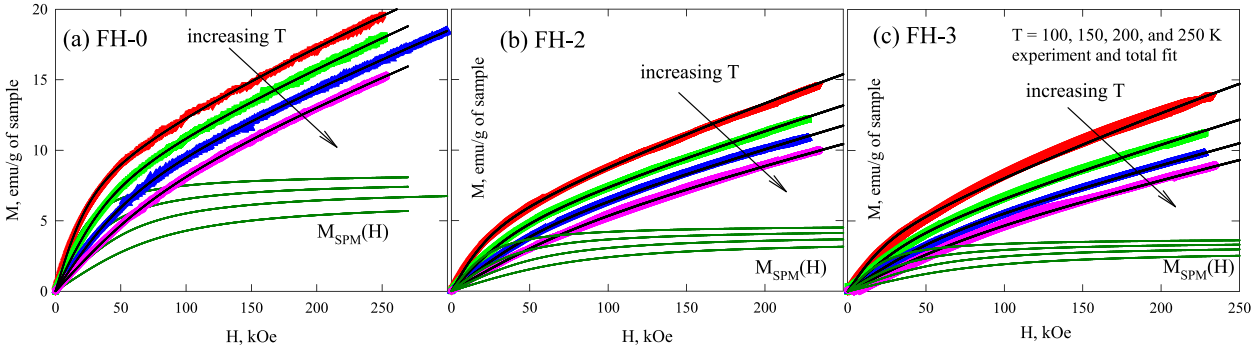

Fig. 1. Experimental magnetization curves (symbols) for samples (a) FH-0, (b) FH-2, and (c) FH-3 at different temperatures (indicated in (c)). The data include the results of the quasi-static measurements on a vibrating sample magnetometer in fields of up to 60 kOe and the results obtained by the pulsed technique in fields of up to 250 kOe. Solid curves show the best fitting by Eq. (2) with allowance for Eqs. (3) and (4), see the text and Table 1. The solid $M_{SPM}(H)$ curves show the partial contribution of the SPM subsystem of the uncompensated particle magnetic moments (the first term in Eq. (2)) to the total magnetization.

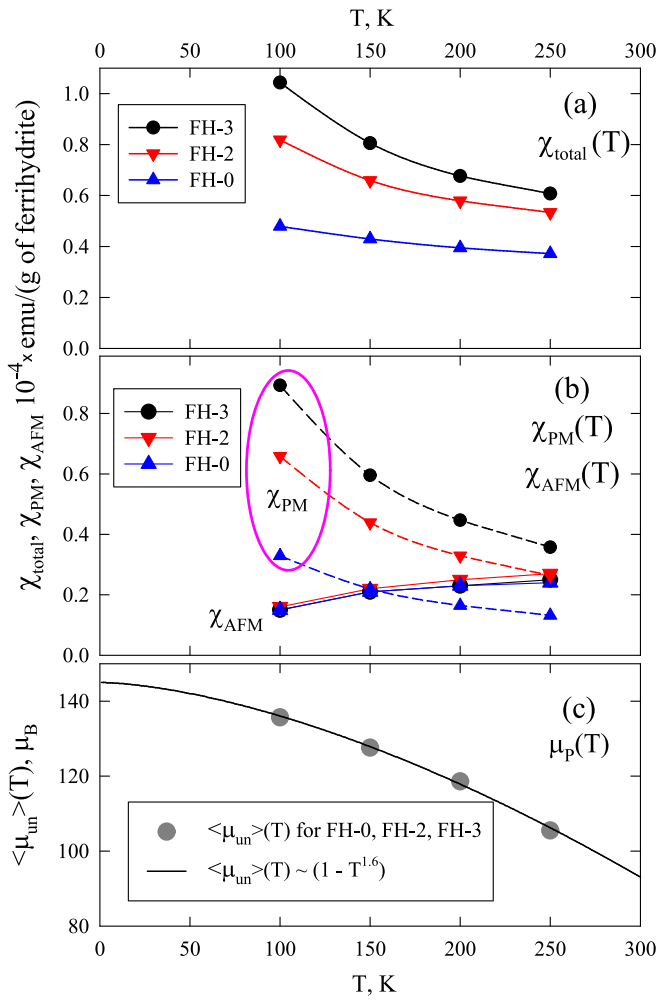

Fig. 2. Temperature dependences of the parameters determined by the processing of the experimental magnetization curves (Fig. 1) obtained for the investigated samples. (a) Parameter χ_{total} (the second term in Eq. (2)). (b) PM susceptibility $\chi_{PM} = M_{PM} \cdot B(H = 10\ kOe)$ derived from the data presented in (a) and AFM susceptibility χ_{AFM}. The data in (a, b) take into account the ferrihydrite mass fraction x in the samples, see Table 1 and the text. (c) Temperature evolution of the uncompensated magnetic moment $< \mu_{un} >$ (symbols) and dependence (7) describing its behavior (solid curve).

temperature. Therefore, a source of the additional contribution to the χ_{total} value should be sought.

If the $\chi_{AFM}(T)$ dependence for the bulk analogue of nanoparticles is known, it should be similar to the $\chi_{AFM}(T)$ dependence obtained by processing of the experimental $M(H)$ dependences at different temperatures for the sample of nanoparticles of the same material. This was previously demonstrated for NiO nanoparticles with average sizes of 23 and 8 nm [31–33,64]. The Néel temperature of ferrihydrite is ~ 350 K [35,38]. However, ferrihydrite has no bulk analogue (a reference sample with submicron particles). In [51], the $\chi_{AFM}(T)$ dependence was calculated within the mean field approximation and the calculation showed no fundamental difference from the generally accepted study of antiferromagnets. At the same time, in some studies of ultrafine particles of various materials with both the antiferro- and ferrimagnetic ordering (see, for example, [31–33,70–78]), it was found that an additional magnetic subsystem forms in particles, in which, at sufficiently high temperatures, the magnetic moments can behave like a paramagnetic (PM) gas. It is reasonable to identify this subsystem with the spins of atoms on the particle surface. Then, in the descending $\chi_{total}(T)$ dependence (Fig. 2a), we can distinguish the susceptibility of the PM subsystem (hereinafter, χ_{PM}), which decreases in inverse proportion to the temperature: $\chi_{PM} \sim 1/T$. In the designations made, we have

$$\chi_{total} = \chi_{PM} + \chi_{AFM}. \quad (5)$$

According to this equation, after extracting the dependences $\chi_{PM}(T) \sim 1/T$ from the data presented in Fig. 2a, it appeared that the $\chi_{AFM}(T)$ dependence is approximately the same for all the samples and increases with temperature (Fig. 2b).

Since, at $T = 100$ and 150 K in fields of more than 150 kOe, the Brillouin function (the $M(H$ dependence) for spin 5/2 (with a g-factor of 2) deviates essentially (by up to 6 % in a field of 250 kOe) from the linear dependence $\chi_{AFM} \cdot H$, then, for the final fitting of the experimental $M(H)$ dependences, it would be more correct to use the Brillouin function $B(H)$. Finally, the magnetization curves were fitted by the equation

$$M(H) = M_{SPM}(H) + M_{PM} \cdot B(H) + \chi_{AFM} \cdot H. \quad (6)$$

Here, M_{PM} is the PM contribution at $T = 0$ (or in the "infinite field"). The results of the best fit using Eq.(6) are shown in Fig. 1 (solid lines). In the processing of the experimental $M(H)$ dependences, the variable temperature-dependent fitting quantities were the parameter n of the $f(\mu_{un})$ distribution function and the χ_{AFM} value. The dispersion s of the $f(\mu_{un})$ distribution function, the number of particles N_P, and the M_{PM} value remained constant for a specific sample at different temperatures. The relative error of the obtained fitting parameters lies within 5 %. The temperature-independent fitting parameters are given in Table 1.

The data presented in Fig. 1 are normalized to the sample mass. The data in Fig. 2a and 2b are normalized to the ferrihydrite mass in the samples at $x_{FH\text{-}1} = 1$, $x_{FH\text{-}2} = 0.56$, and $x_{FH\text{-}3} = 0.45$. Fig. 2b shows the χ_{PM} values (in this case, $\chi_{PM} = M_{PM} \cdot B(H = 10\ kOe)$) and the χ_{AFM} values at different temperatures. It can be seen that the $\chi_{AFM}(T)$ dependences are approximately the same and coincide well for all the samples; these are the dependences that increase with temperature, as predicted for an antiferromagnet with a random distribution of the crystallographic axes.

The temperature evolution of the average uncompensated magnetic moment $< \mu_{un} >$ is presented in Fig. 2c. This dependence obeys the power law

$$< \mu_{un} > (T) = < \mu_{un} > (T = 0) \cdot (1 - const \cdot T^a) \quad (7)$$

at $a \approx 1.6$ and a similar power law is frequently observed in AFM nanoparticle systems [10,11,32,33,42–44,49,50,53,64,79,80]. Using functional dependence (7), one can obtain a quite accurate value of $< \mu_{un} > (T = 0) = 145\ \mu_B$ (μ_B is the Bohr magneton). The corresponding $f(\mu_{un})$ distribution function at $s = 0.1$ is shown in the inset to Fig. 3.

Let us compare the $f(\mu_{un})$ function and particle size distribution. According to Néel's hypothesis [5], the μ_{un} value can be estimated as

$$m_{un} \sim m_{at} \cdot N_{at}^b. \quad (8)$$

Here, N_{at} is the number of magnetically active atoms in a particle, μ_{at} is the magnetic moment of the atom, and the exponent b is 1/3 if defects emerge on the particle surface, 1/2 if they are present in the bulk of a particle, and 2/3 if there is an odd number of planes with the parallel spins in a particle. In several studies, it was established by comparing the $< \mu_{un} >$ and $< d >$ values that the exponent b for ferrihydrite is close to 1/2 [36,37,43,44,47–50,61,79,80].

At the average distance $d_{Fe\text{-}Fe}$ (~0.3 nm for ferrihydrite [37]) between iron atoms, the number N_{Fe} of iron atoms in a particle is

$$N_{Fe} \approx f \cdot \{(d/d_{Fe-Fe}) + 1\}^3,$$

where the coefficient f is unity for a cubic particle and $f \approx \pi/6$ for spherical one and d is the particle size. Combining this equation with Néel equation (8) at $N_{at} = N_{Fe}$ and $\mu_{at} = \mu_{Fe}$, we arrive at

$$d(\mu_{un}) = d_{Fe\text{-}Fe} \cdot \left\{ \left(\frac{\mu_{un}}{\mu_{Fe}} \right)^{\frac{1}{3b}} \cdot \frac{1}{f^{1/3}} - 1 \right\} \quad (9)$$

Table 1
Parameters used in fitting the magnetization curves (Fig. 1) that ensure the best agreement between the experiment and calculation using Eq. (6) at the identical $f(\mu_{un})$ distributions for all the samples.

Sample	x, mass fraction of ferrifydrite	M_{SPM} parameters N_P per g of the sample	N_P per g of ferrihydrite	s	$<\mu_P(T=0)>$, μ_B	M_{PM} parameters M_{PM}, emu/(g of the sample)	M_{PM}, emu/(g of ferrihydrite)
FH-0	1.0	$6.7 \cdot 10^{18}$	$6.7 \cdot 10^{18}$	0.1	145	21	21
FH-2	0.56	$3.75 \cdot 10^{18}$	$6.7 \cdot 10^{18}$	0.1	145	23.5	42
FH-3	0.45	$3.02 \cdot 10^{18}$	$6.7 \cdot 10^{18}$	0.1	145	18.9	57

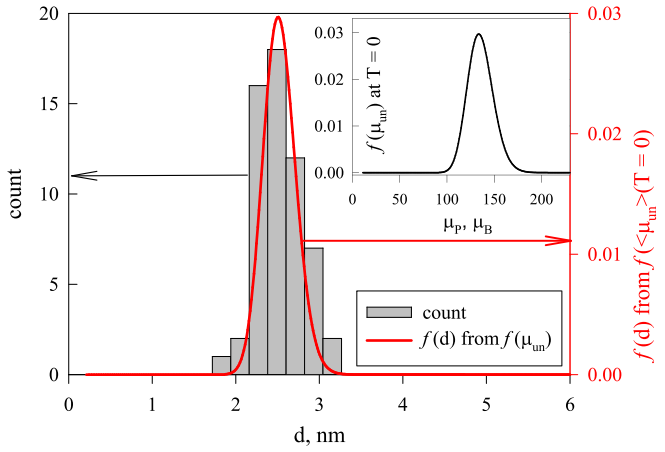

Fig. 3. Ferrihydrite nanoparticle size distribution histogram (the ordinate axis on the left) and corresponding particle size distribution function $f(d)$ (the y axis on the right) obtained from the $f(\mu_{un})$ function (at the parameters corresponding to $T = 0$ K, see Table 1 and the text in Subsection 3.1.) through Eq. (9). Inset: $f(\mu_{un})$ function at $T = 0$ K.

The $f(\mu_{un})$ distribution function (at $T = 0$) reconstructed according to Eq. (9) agrees well with the particle size distribution at $b \approx 0.485$ for f = 1 and $b \approx 0.535$ for f = $\pi/6$. This is illustrated in Fig. 3, where the particle size distribution histogram is compared with the $f(d)$ function (the y axis on the right) obtained from the $f(\mu_{un})$ function. The exponent b in Eq. (8) is very close to 1/2, which indicates that the uncompensated moment is induced by defects both on the surface and in the bulk of particles. It can be established from the value $<\mu_{un}>(T = 0) = 145\ \mu_B$ that the uncompensated moment is formed by approximately 30 magnetic moments of iron (at $\mu_{at} = \mu_{Fe3+} \approx 5\ \mu_B$).

3.2. Quantitative estimation of the magnetic subsystems and model of the magnetic state of ferrihydrite particles

Thus, the analysis of the $M(H)$ dependences showed good agreement of the uncompensated magnetic moment with the Néel's model hypothesis and, taking into account the PM contribution, made it possible to extract the temperature behavior of the AFM susceptibility $\chi_{AFM}(T)$ consistent with the general approach from the temperature evolution of the parameter χ_{total}. Based on these facts, which allow us to state the adequacy of the fitting parameters obtained, we make the quantitative estimations for the magnetic subsystems forming in ferrihydrite nanoparticles.

A ferrihydrite particle 2.7 nm size (this is the $< d >$ value for the investigated systems) contains, in the ideal cubic shape approximation, $\sim 10^3$ of iron atoms, half of which are located on the surface and half, in the bulk of a particle; about 100 atoms are located on the edges of a regular cube. In a spherical particle $< d > = 2.7$ nm in diameter, we have $N_{Fe} \approx 700$ and the number of surface iron atoms ($\sim$380) is somewhat higher than the number of internal iron atoms ($\sim$320). A pronounced habit can hardly be expected for such fine ferrihydrite particles, which was confirmed by the TEM data [65,66]. It is reasonable to assume that real particles have a shape intermediate between a cube (f = 1) and a sphere (f = $\pi/6$). In a particle of intermediate shape, the edge between faces should rather be understood as the outermost atoms of the atomic planes emerging on the surface or protruding areas of particles. The number of such atoms in a particle with the shape intermediate between a cube and a sphere is most likely expected to be somewhat larger than 100 atoms mentioned for the cube edges. A number of the uncompensated magnetic moments of atoms (30) is significantly smaller than the number of atoms on the surface and in the bulk and atoms on protruding particle areas, which additionally evidences for the statistical distribution of defects, both on the surface and in the bulk of particles (according to the Néel's hypothesis).

Let us estimate atoms that form the PM subsystem from the obtained M_{PM} values (last column in Table 1). According to the nominal chemical formula $5Fe_2O_3 \cdot 9H_2O$ of ferrihydrite, the mass fraction of iron is $X_{Fe} \approx 0.58$; we use this value to recalculate the PM magnetization of the M_{PM} subsystem in emu units reduced to the iron mass (more precisely, the iron ion mass) in the sample. A simple calculation shows that, in sample FH-0, a value of $M_{PM} = 21$ emu/g of ferrihydrite corresponds to ~ 7 % of the total number N_{Fe} of iron atoms or corresponds to ~ 70 iron atoms in a particle of ideal cubic shape (50 atoms for a spherical shape). The similar estimations for samples FH-2 and FH-3 yield the following results: the fraction of PM atoms is approximately 15 % and 20 % of the N_{Fe} value and their number is approximately 150 and 200 for the cubic shape and 100 and 140 for the spherical shape in samples FH −2 and FH-3, respectively. A reasonable value of the possible deviation of the iron mass fraction X_{Fe} from the nominal chemical formula of ferrihydrite can be indicated as 10–15 %. This value determines the probable source of error in determining the number of PM atoms in a particle. However, due to the identity of the properties of particles in the samples (see Subsection 2.1), this estimation error is the same for all the samples under study.

The estimated numbers of PM atoms indicate that not all surface iron atoms in a ferrihydrite nanoparticle are paramagnetic, even taking into account an X_{Fe} error of 10–15 %. It can be stated that the number of PM atoms corresponds to the number of iron atoms in protruding areas ("edges") of particles, taking into account that, for the particle shape intermediate between a cube and a sphere, a number of atoms on the "edges" (protruding areas) is expected to be somewhat greater than a calculated value of 100 atoms of the cube (see above). A similar result was obtained when studying NiO nanoparticles in [31,64], where it was concluded that paramagnetic nickel atoms are located mainly on the edges or protruding areas of particles.

The largest part of the magnetic moments of iron in a particle, which remained after taking into account the magnetic moments of iron atoms forming the uncompensated particle moment and PM atoms, is ordered antiferromagnetically. If we recalculate the χ_{AFM} values (Fig. 2b) to the mass fraction X_{Fe} of iron in ferrihydrite ($X_{Fe} \approx 0.58$), then, taking into account the inevitable uncertainty in the determination of X_{Fe}, they are in satisfactory agreement with the results reported in [51]. For example, in our case, $\chi_{AFM} \approx 0.26 \cdot 10^{-4}$ emu/(Oe $\cdot$ g_{Fe}) at 100 K and, in [51], at the same temperature, $\chi_{AFM} \approx 0.4 \cdot 10^{-4}$ emu/(Oe $\cdot$ g_{Fe}) within the mean field theory.

A surprising result was a significant increase in the fraction of PM atoms with the increasing degree of coating of ferrihydrite particles (see

Fig. 2b and the last column in Table 1), while the SPM response (uncompensated moment) recalculated to the ferrihydrite mass was identical for all the samples and the AFM susceptibility was approximately the same.[1] In principle, an additional coating of a nanoparticle should modify its initial surface and, in many cases, such modification also changes the magnetic properties of particles (see, for example, [81–84]). It can be assumed that, in initial sample FH-0, there are chemical bonds (the wave function overlap) between (iron) atoms of neighboring particles and, in AG-coated ferrihydrite particles, these bonds are broken. This fairly bold assumption is consistent with the results of the analysis of the origin of the strong interparticle magnetic interactions in ferrihydrite powder systems. For example, the difference between the temperatures of the transition to the SPM state in samples FH-0 and FH-3 is more than 30 degrees ($T_B = 18.3$ K for sample FH-3 and $T_B = 49$ K for sample FH-0) [65,67]. Taking into account the identity of the sizes and uncompensated magnetic moments of particles, this growth of the SPM blocking temperature is related to the interparticle magnetic interactions. At the same time, the dipole–dipole interaction energy in initial synthetic ferrihydrite (sample FH-0) is only a few degrees [65,67], which cannot explain such a significant increase in the characteristic temperature T_B. Then, it is natural to attribute the strong interparticle magnetic interactions to the exchange or superexchange between atoms of neighboring particles that are in close contact. In this case, the atoms involved in the exchange will not exhibit the PM behavior. At the spatial separation of particles, these bonds will be broken and the number of PM atoms, which are located mainly in protruding areas, will increase. This is qualitatively consistent with the obtained result on an increase in the PM contribution in the FH-0, FH-2, and FH-3 sample series. It should be noted that the exchange couplings between atoms of neighboring particles as a possible cause for the fairly strong interparticle magnetic interactions in AFM nanoparticle systems were proposed in review [26]. The described picture is schematically shown in Fig. 4, which presents two individual particles (Fig. 4a) and two particles in close contact with each other (Fig. 4b). In the second case, some atoms on the protruding parts of particles become associated with atoms of a neighboring particle and their magnetic moments are no longer free (paramagnetic).

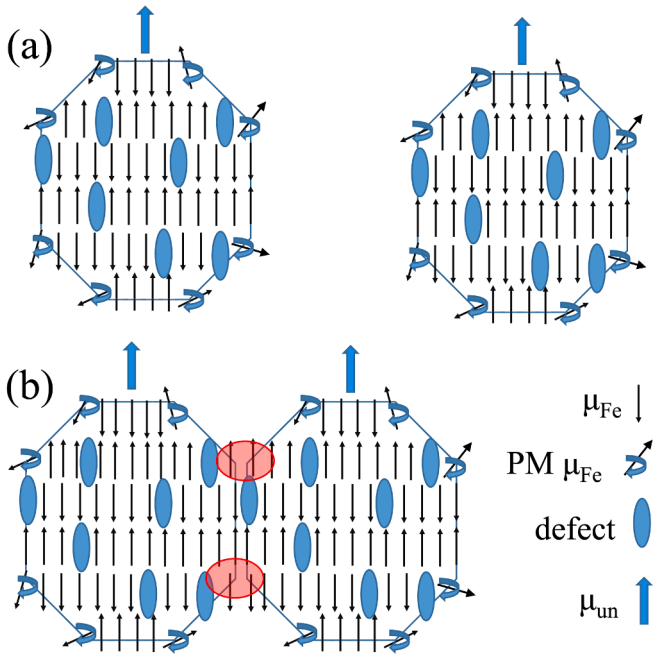

Fig. 4. Schematic of magnetic subsystems in AFM nanoparticles of the investigated ferrihydrite systems. (a) Spatially separated particles (samples FH-2 and FH-3) and (b) closely contacting particles (sample FH-0). Designations for the magnetic moments μ_{Fe} of iron atoms, defects, uncompensated moments μ_{un} of particles (the vectors μ_{un} can be parallel if a field is sufficiently strong), and free (PM) magnetic moments are presented in (b). Red ovals in (b) correspond to the possible exchange coupling between iron atoms of neighboring closely contacting particles. The octagonal shape of particles is used to emphasize that there are protruding areas on real particles, in which PM iron atoms are mainly located.

4. Conclusions

The analysis of the magnetization curves of the systems with different degrees of AG coating of ferrihydrite nanoparticles in fields of up to 250 kOe suggested a model of the magnetic state of AFM ferrihydrite nanoparticles with an average size of ~ 2.7 nm. Within this model, the magnetic moment of particles is formed by decompensated spins of iron atoms due to defects located partially on the surface of a particle, as well as in the bulk of it; Néel's relation (8) is satisfied at $b \approx 0.5 \pm 0.03$. The fraction of spins of all iron atoms in a particle in this subsystem is ~ 3 % and their number is about 30, which determines an average uncompensated particle moment of ~ 150 Bohr magnetons.

The field-linear contribution to the total magnetization is caused by the response from the AFM particle core and the PM behavior of a part of the surface spins unrelated to the exchange coupling with the AFM core. The fraction of these free (paramagnetic) spins depends on the degree of spatial separation of ferrihydrite particles and increases from ~ 7 % for the initial sample (FH-0) without nanoparticle coating to ~ 20 % for the sample with the highest degree of AG coating (FH-3). These facts lead to two conclusions. The number of PM spins in a particle is significantly less than the number of spins on the particle surface, i.e., the free (PM) magnetic moments of iron atoms are located mainly on the protruding areas of particles. The growing fraction of PM spins in the sample series FH-0, FH-2, and FH-3 is apparently related to the formation of exchange couplings between the surface iron atoms of neighboring particles and the destruction of these couplings upon AG coating of ferrihydrite particles. These couplings may cause the strong impact of the interparticle magnetic interactions on the SPM blocking temperature in initial synthetic ferrihydrite [62,64]. When particles are spatially separated, these couplings are destroyed (the intensity of the interparticle interactions decreases) and the number of free PM spins grows.

The AFM ordering is preserved over almost the entire particle volume; it is formed by about 90–75 % of the magnetic moments of iron atoms. The use of a wide range of external fields made it possible to correctly extract the contribution corresponding to the antiferromagnetic susceptibility of ferrihydrite. A significant progression of this work from the previous studies on the ferrihydrite and ferritin systems is that the presented analysis yielded the $\chi_{AFM}(T)$ dependence increasing with temperature that is typical of an antiferromagnet.

Funding

This study was supported by his work was supported by the Russian Science Foundation, project no. 22–72-00134.

[1] As the number of PM spins (for spatially separated particles) increases, one can expect a slight decrease in the AFM susceptibility (and vice versa). The rough estimate is approximately a 10% increase in the χ_{AFM} value for sample FH-3 as compared with sample FH-0. This is at the level of the χ_{AFM} determination error and it should be noted that there can be another contribution to the susceptibility of a nano-antiferromagnet that is known as the superantiferromagnetic susceptibility [6]. This contribution comes from the additional canting of the spin planes extreme to the particle surface in an external field, if the number of these ferromagnetically ordered planes in an AFM particle is odd [6,49,51]. As was shown in [51], for ferrihydrite about 3–5 nm in size, this contribution can be clearly distinguished only in strong fields exceeding those used in this work. By χ_{AFM}, the authors mean the ordinary susceptibility of an antiferromagnet, including the possible contribution of the described excess superantiferromagnetic susceptibility.

CRediT authorship contribution statement

A.A. Krasikov: Software, Investigation, Funding acquisition, Data curation. **D.A. Balaev:** . **A.D. Balaev:** Writing – review & editing, Methodology, Investigation. **S.V. Stolyar:** Supervision, Methodology, Conceptualization. **R.N. Yaroslavtsev:** Investigation. **R.S. Iskhakov:** Writing – review & editing, Supervision, Conceptualization.

Declaration of competing interest

The authors declare the following financial interests/personal relationships which may be considered as potential competing interests: Aleksandr Krasikov reports financial support was provided by Russian Science Foundation. If there are other authors, they declare that they have no known competing financial interests or personal relationships that could have appeared to influence the work reported in this paper.

Data availability

Data will be made available on request.

Acknowledgments

Authors thank to D.A. Velikanov, S.V. Komogortsev for fruitful discussions.

References

[1] C.h. Kittel, Physical theory of ferromagnetic domains, Rev. Mod. Phys. 21 (N4) (1949) 541–583, https://doi.org/10.1103/RevModPhys.21.541.
[2] L. Néel, Theorie du trainage magnetique des ferromagnetique en grains fins avec applications aux terres cuites, Ann. Geophys. 5 (1949) 99–136.
[3] C.P. Bean, I.S. Jacobs, Magnetic Granulometry and Super-Paramagnetism, J. Appl. Phys. 27 (1956) 1448–1452, https://doi.org/10.1063/1.1722287.
[4] C.P. Bean, I.S. Jakobs, Magnetic Granulometry and Super-Paramagnetism, J. Appl. Phys. 27 (1956) 1448, https://doi.org/10.1063/1.1722287.
[5] L. Néel, Superantiferromagnetism in small particles, CR Acad. Sci. Paris 253 (1961) 203.
[6] L. Néel, Sur le calcul de la susceptibilité additionnelle super-antiferromagnétique des grains fins et sa variation thermique, C.R, Acad. Sci. Paris 253 (1961) 1286.
[7] F.E. Luborsky, Development of Elongated Particle Magnets, J. Appl. Phys. 32, S171–S183 (1961). doi.org/10.1063/1.2000392.
[8] W.F. Brown, Thermal Fluctuations of a Single-Domain Particle, Phys. Rev. 130 (1963) 1677–1686.
[9] J.P. Chen, C.M. Sorensen, K.J. Klabunde, G.C. Hadjipanayis, E. Devlin, A. Kostikas, Size-dependent magnetic properties of $MnFe_2O_4$ fine particles synthesized by coprecipitation, Phys. Rev. B 54 (13) (1996) 9288, https://doi.org/10.1103/PhysRevB.54.9288.
[10] C. Martínez-Boubeta, K. Simeonidis, M. Angelakeris, N. Pazos-Pérez, M. Giersig, A. Delimitis, L. Nalbandian, V. Alexandrakis, D. Niarchos, Critical radius for exchange bias in naturally oxidized Fe nanoparticles, Phys. Rev. B 74 (2006) 054430, https://doi.org/10.1103/PhysRevB.74.054430.
[11] M. Knobel, W.C. Nunes, L.M. Socolovsky, E. De Biasi, J.M. Vargas, J.C. Denardin, Superparamagnetism and other magnetic features in granular materials: a review on ideal and real systems, J. Nanosci. Nanotechnol. 8 (2008) 2836–2857, https://doi.org/10.1166/jnn.2008.017.
[12] Y. Jun,J Seo, J. Cheon,, Nanoscaling laws of magnetic nanoparticles and their applicabilities in biomedical sciences, Acc. Chem. Res. 41 (2) (2008) 179–189, https://doi.org/10.1021/ar700121f.
[13] A.G. Kolhatkar, A.C. Jamison, D. Litvinov, R.C. Willson, T.R. Lee, Tuning the Magnetic Properties of Nanoparticles, Int. J. Mol. Sci. 14 (2013) 15977–16009, https://doi.org/10.3390/ijms140815977.
[14] J. Mohapatra, M. Xing, J.P. Liu, Inductive thermal effect of ferrite magnetic nanoparticles, Mater. 19 (2019) 3208, https://doi.org/10.3390/ma12193208.
[15] X. Batlle, C. Moya, M. Escoda-Torroella, Ò. Iglesias, A.F. Rodríguez, A. Labarta, Magnetic nanoparticles: from the nanostructure to the physical properties, J. Magn. Magn. Mater. 543 (2022) 168594, https://doi.org/10.1016/j.jmmm.2021.168594.
[16] S.I. Ahmad, Nano cobalt ferrites: doping, structural, low-temperature, and room temperature magnetic and dielectric properties – a comprehensive review, J. Magn. Magn. Mater. 562 (2022) 169840, https://doi.org/10.1016/j.jmmm.2022.169840.
[17] A. Aharoni, Surface anisotropy in micromagnetics, J. Appl. Phys. 61 (1987) 3302–3304, https://doi.org/10.1063/1.338890.
[18] F. Bødker, S. Mørup, S. Linderoth, Surface EH'ects in Metallic Iron Nanoparticles, Phys. Rev. Lett. 72 (1994) 282–285, https://doi.org/10.1103/PhysRevLett.72.282.
[19] V.P. Shilov, J.-C. Bacri, F. Gazeau, F. Gendron, R. Perzynski, Y.L. Raikher, V. P. Shilov, et al., Ferromagnetic resonance in ferrite nanoparticles with uniaxial surface anisotropy, J. Appl. Phys. 85 (1999) 6642, https://doi.org/10.1063/1.370173.
[20] M. Tadic, D. Nikolić, M. Panjan, G.R. Blake, Magnetic properties of NiO (nickel oxide) nanoparticles: Blocking temperature and Neel temperature, J. Alloy. Compd. 647 (2015) 1061, https://doi.org/10.1016/j.jallcom.2015.06.027.
[21] S. Oyarzún, A. Tamion, F. Tournus, V. Dupuis, M. Hillenkamp, Size effects in the magnetic anisotropy of embedded cobalt nanoparticles: from shape to surface, Sci. Rep. 5 (1) (2015) 14749, https://doi.org/10.1038/srep14749.
[22] J. Mohapatra, M. Xing, J. Elkins, J. Beatty, J. Ping Liu, J. Mohapatra, et al., Size-dependent magnetic hardening in $CoFe_2O_4$ nanoparticles: effects of surface spin canting, J. Phys. D Appl. Phys. 53 (2020) 504004.
[23] Y.V. Knyazev, D.A. Balaev, V.L. Kirillov, O.A. Bayukov, O.N. Mart'yanov, Knyazev, Yu V.,, et al., Mössbauer spectroscopy study of the superparamagnetism of ultrasmall ϵ-Fe_2O_3 nanoparticles, JETP Lett. 108 (2018) 527, https://doi.org/10.1134/S0021364018200092.
[24] D.A. Balaev, I.S. Poperechny, A.A. Krasikov, S.V. Semenov, S.I. Popkov, Y. V. Knyazev, V.L. Kirillov, S.S. Yakushkin, O.N. Martyanov, Y.L. Raikher, Dynamic remagnetisation of $CoFe_2O_4$ nanoparticles: thermal fluctuational thawing of anisotropy, J. Phys. D Appl. Phys. 54 (2021) 275003, https://doi.org/10.1088/1361-6463/abf371.
[25] D.A. Balaev, A.A. Dubrovskiy, Y.V. Knyazev, S.V. Semenov, V.L. Kirillov, O. N. Martyanov, The manifestation of surface and size effects in the magnetic properties of ε-Fe2O3 nanoparticles. (Brief overview), Phys. Solid State 65, (N6) (2023) 938–946, https://doi.org/10.21883/PSS.2023.06.56105.12H.
[26] S. Mørup, D.E. Madsen, C. Fradsen, C.R.H. Bahl, M.F. Hansen, Experimental and theoretical studies of nanoparticles of antiferromagnetic materials, J. Phys.: Condens. Matter 19, 213202 (2007). https://doi.org/10.1088/0953-8984/19/21/213202.
[27] A. Punnoose, H. Magnone, M.S. Seehra, J. Bonevich, Bulk to nanoscale magnetism and exchange bias in CuO nanoparticles, Phys. Rev. B 64 (2001) 174420, https://doi.org/10.1103/PhysRevB.64.174420.
[28] C.R.H. Bahl, M.F. Hansen, T. Pedersen, S. Saadi, K.H. Nielsen, B. Lebech, S. Mørup, The magnetic moment of NiO nanoparticles determined by Mössbauer spectroscopy, J. Phys. Condens. Matter 18 (2006) 4161–4175, https://doi.org/10.1088/0953-8984/18/17/005.
[29] M. Tadić, M. Panjan, D. Marković, NiO/SiO_2 nanostructure and the magnetic moment of NiO nanoparticles, Mater. Lett. 64 (2010) 2129–2131, https://doi.org/10.1016/j.matlet.2010.07.006.
[30] S.D. Tiwari, K.P. Rajeev, Effect of distributed particle magnetic moments on the magnetization of NiO nanoparticles, Solid State Commun. 152 (2012) 1080, https://doi.org/10.1016/j.ssc.2012.03.003.
[31] S.I. Popkov, A.A. Krasikov, A.A. Dubrovskiy, M.N. Volochaev, V.L. Kirillov, O. N. Martyanov, D.A. Balaev, Size effects in the formation of an uncompensated ferromagnetic moment in NiO nanoparticles, J. Appl. Phys. 126 (2019) 103904, https://doi.org/10.1063/1.5109054.
[32] S.I. Popkov, A.A. Krasikov, D.A. Velikanov, V.L. Kirillov, O.N. Martyanov, D. A. Balaev, Formation of the magnetic subsystems in antiferromagnetic NiO nanoparticles using the data of magnetic measurements in fields up to 250 kOe, J. Magn. Magn. Mater. 483 (2019) 21, https://doi.org/10.1016/j.jmmm.2019.03.004.
[33] D.A. Balaev, A.A. Krasikov, S.I. Popkov, S.V. Semenov, M.N. Volochaev, D. A. Velikanov, V.L. Kirillov, O.N. Martyanov, Uncompensated magnetic moment and surface and size effects in few-nanometer antiferromagnetic NiO particles, J. Magn. Magn. Mater. 539 (2021) 168343, https://doi.org/10.1016/j.jmmm.2021.168343.
[34] T. Iimor, Y. Imamoto, N. Uchida, Y. Kikuchi, K. Honda, T. Iwahashi, Y. Ouch, Magnetic moment distribution in nanosized antiferromagnetic NiO, J. Appl. Phys. 127 (2020) 023902, https://doi.org/10.1063/1.5135335.
[35] M. Seehra, V.S. Babu, A. Manivannan, J. Lynn, Neutron scattering and magnetic studies of ferrihydrite nanoparticles, Phys. Rev. B 61 (5) (2000) 3513–3518, https://doi.org/10.1103/PhysRevB.61.3513.
[36] J.G.E. Harris, J.E. Grimaldi, D.D. Awschalom, A. Chiolero, D. Loss, Excess spin and the dynamics of antiferromagnetic ferritin, Phys. Rev. B 60 (1999) 3453–3456, https://doi.org/10.1103/PhysRevB.60.3453.
[37] A. Punnoose, T. Phanthavady, M. Seehra, N. Shah, G. Huffman, Magnetic properties of ferrihydrite nanoparticles doped with Ni, Mo, and Ir, Phys. Rev. B 69 (5) (2004) 054425, https://doi.org/10.1103/PhysRevB.69.054425.
[38] M.S. Seehra, V. Singh, X. Song, S. Bali, E.M. Eyring, Synthesis, structure and magnetic properties of non-crystalline ferrihydrite nanoflakes, J. Phys. Chem. Solid 71 (2010) 1362–1366, https://doi.org/10.1016/j.jpcs.2010.06.003.
[39] C.h. Rani, S.D. Tiwari, Superparamagnetic behavior of antiferromagnetic six lines ferrihydrite nanoparticles, Phys. B 513 (2017) 58, https://doi.org/10.1016/j.physb.2017.02.036.
[40] C. Rani, S. Tiwari, Estimation of particle magnetic moment distribution for antiferromagnetic ferrihydrite nanoparticles, Journ. Magn. Magn Mater. 385 (2015) 272–276, https://doi.org/10.1016/j.jmmm.2015.02.048.
[41] D.A. Balaev, A.A. Krasikov, A.A. Dubrovskiy, S.I. Popkov, S.V. Stolyar, O. A. Bayukov, R.S. Iskhakov, V.P. Ladygina, R.N. Yaroslavtsev, Magnetic properties of heat treated bacterial ferrihydrite nanoparticles, Journ. Magn. Magn. Mater. 410 (2016) 71, https://doi.org/10.1016/j.jmmm.2016.02.059.
[42] Y. Guyodo, S.K. Banerjee, R. Lee Penn, D. Burleson, T.S. Berquo, T. Seda, P. Solheid, Magnetic properties of synthetic six-line ferrihydrite nanoparticles, Phys. Earth Planet. In. 154 (2006) 222–233, https://doi.org/10.1016/j.pepi.2005.05.009.
[43] Y.V. Knyazev, D.A. Balaev, S.V. Stolyar, A.A. Krasikov, O.A. Bayukov, M. N. Volochaev, R.N. Yaroslavtsev, V.P. Ladygina, D.A. Velikanov, R.S. Iskhakov,

Interparticle magnetic interactions in synthetic ferrihydrite: Mössbauer spectroscopy and magnetometry study of the dynamic and static manifestations, J. Alloy. Compd. 889 (2021) 161623, https://doi.org/10.1016/j.jallcom.2021.161623.
[44] S.V. Stolyar, D.A. Balaev, V.P. Ladygina, A.A. Dubrovskiy, A.A. Krasikov, S. I. Popkov, O.A. Bayukov, Y.V. Knyazev, R.N. Yaroslavtsev, M.N. Volochaev, R. S. Iskhakov, K.G. Dobretsov, E.V. Morozov, O.V. Falaleev, E.V. Inzhevatkin, O. A. Kolenchukova, I.A. Chizhova, Bacterial ferrihydrite nanoparticles: preparation, magnetic properties, and application in medicine, J. Supercond. Nov. Magn. 31 (2018) 2297, https://doi.org/10.1007/s10948-018-4700-1.
[45] C. Rani, S.D. Tiwari, Magnetic Properties of Two Lines Ferrihydrite Nanoparticles, Physica Status Solidi (b) 259 (11) (2022) 2200251, https://doi.org/10.1002/pssb.202200251.
[46] C. Rani, S.D. Tiwari, Temperature variation of surface magnetization in antiferromagnetic six lines ferrihydrite nanoparticles, J. Magn. Magn. Mater. 587 (2023) 171341, https://doi.org/10.1016/j.jmmm.2023.171341.
[47] S.A. Makhlouf, F.T. Parker, A.E. Berkowitz, Magnetic hysteresis anomalies in ferritin, Phys. Rev. B 55 (1997) R14717, https://doi.org/10.1103/PhysRevB.55.R14717.
[48] C. Gilles, P. Bonville, K.K.W. Wong, S. Mann, Non-Langevin behaviour of the uncompensated magnetization in nanoparticles of artificial ferritin, Eur. Phys. J. B 17 (2000) 417–427.
[49] C. Gilles, P. Bonville, H. Rakoto, J.M. Broto, K.K.W. Wong, S. Mann, Magnetic hysteresis and superantiferromagnetism in ferritin nanoparticles, J. Magn. Magn. Mater. 241 (2002) 430, https://doi.org/10.1016/S0304-8853(01)00461-9.
[50] N.J.O. Silva, V.S. Amaral, L.D. Carlos, Relevance of magnetic moment distribution and scaling law methods to study the magnetic behavior of antiferromagnetic nanoparticles: Application to ferritin, Phys. Rev. B 71 (2005) 184408, https://doi.org/10.1103/PhysRevB.71.184408.
[51] N.J.O. Silva, A. Millan, F. Palacio, E. Kampert, U. Zeitler, V.S. Amaral, Temperature dependence of antiferromagnetic susceptibility in ferritin, Phys. Rev. B 79 (2009) 104405, https://doi.org/10.1103/PhysRevB.79.104405.
[52] R.P. Guertin, N. Harrison, Z.X. Zhou, S. McCall, F. Drymiotis, Very high field magnetization and AC susceptibility of native horse spleen ferritin, J. Magn. Magn. Mater. 308 (2007) 97, https://doi.org/10.1016/j.jmmm.2006.05.010.
[53] L. Bossoni, J.A. Labra-Munõz, H.S.J. van der Zant, V. Călukovic, A. Lefering, R. Egli, M. Huber, In-depth magnetometry and EPR analysis of the spin structure of human-liver ferritin: from DC to 9 GHz, PCCP 25 (2023) 27694–27717, https://doi.org/10.1039/d3cp01358h.
[54] S.A. Makhlouf, Magnetic properties of Cr_2O_3 Nanoparticles, J. Magn. Magn. Mater. 272–276 (2004) 1530–1532, https://doi.org/10.1016/S0304-8853(03)01576-2.
[55] M. Tadic, I. Milosevic, S. Kralj, M. Mbodji, L. Motte, Silica-Coated and Bare Akaganeite Nanorods: Structural and Magnetic Properties, J. Phys. Chem. C 119 (2015) 13868–13875, https://doi.org/10.1021/acs.jpcc.5b01547.
[56] M. Tadic, I. Milosevic, S. Kralj, M.-L. Saboung, L. Motte, Ferromagnetic behavior and exchange bias effect in akaganeite nanorods, Applied Physics Letters 106, (N18), 183706 (2015). dx.doi.org/10.1063/1.4918930.
[57] E.V. Inzhevatkin, O.A. Kolenchukova, K.G. Dobretsov, V.P. Ladygina, A. V. Boldyreva, S.V. Stolyar, Efficiency of ampicillin-associated biogenic ferrihydrite nanoparticles in combination with a magnetic field for local treatment of burns, Bull. Exp. Biol. Med. 169 (2020) 683–686, https://doi.org/10.1007/s10517- 020-04954-y.
[58] S.V. Stolyar, V.P. Ladygina, A.V. Boldyreva, O.A. Kolenchukova, A.M. Vorotynov, M.S. Bairmani, R.N. Yaroslavtsev, R.S. Iskhakov, Synthesis, properties, and in vivo testing of biogenic ferrihydrite nanoparticles, Bull. Russ. Acad. Sci. Phys. 84 (11) (2020) 1366–1369, https://doi.org/10.3103/S106287382011026X.
[59] S.V. Stolyar, O.A. Kolenchukova, A.V. Boldyreva, N.S. Kudryasheva, Y. V. Gerasimova, A.A. Krasikov, R.N. Yaroslavtsev, O.A. Baykov, V.P. Ladygina, R. S. Iskhakov, Biogenic ferrihydrite nanoparticles: synthesis, properties in vitro and in vivo testing and the concentration effect, Biomedicines 9 (2021) 323, https://doi.org/10.3390/biomedicines9030323.
[60] D.E. Madsen, S. Morup, M.F. Hansen, On the interpretation of magnetization data for antiferromagnetic nanoparticles, Journ. of Magnetism and Magnetic Materials 305 (2006) 95–99, https://doi.org/10.1016/j.jmmm.2005.11.033.
[61] S. Morup, C. Fradsen, Thermoinduced Magnetization in Nanoparticles of Antiferromagnetic Materials, Phys. Rev. Lett. 92 (2004) 21720, https://doi.org/10.1103/PhysRevLett.92.217201.
[62] N.J.O. Silva, L.D. Carlos, V.S. Amaral, Comment on "Thermoinduced Magnetization in Nanoparticles of Antiferromagnetic Materials, Phys. Rev. Lett. 94 (2005) 039707, https://doi.org/10.1103/PhysRevLett.94.039707.
[63] S. Morup, C. Fradsen, Mørup and Frandsen Reply, Phys. Rev. Lett. 94 (2005) 039708, https://doi.org/10.1103/PhysRevLett.94.039708.
[64] A.A. Krasikov, D.A. Balaev, Analysis of Magnetization Processes in Antiferromagnetic Nanoparticles in Strong Pulse Fields (Brief Review), J. Exp. Theor. Phys. 136 (1) (2023) 97–105, https://doi.org/10.1134/S1063776123010132.
[65] A.A. Krasikov, Y.V. Knyazev, D.A. Balaev, D.A. Velikanov, S.V. Stolyar, Y. L. Mikhlin, R.N. Yaroslavtsev, R.S. Iskhakov, Interparticle magnetic interactions and magnetic field dependence of superparamagnetic blocking temperature in ferrihydrite nanoparticle powder systems, Phys. B 660 (2023) 414301, https://doi.org/10.1016/j.physb.2023.414901.
[66] Y.V. Knyazev, D.A. Balaev, R.N. Yaroslavtsev, A.A. Krasikov, D.A. Velikanov, Y. L. Mikhlin, M.N. Volochaev, O.A. Bayukov, S.V. Stolyar, R.S. Iskhakov, Tuning the interparticle interactions in ultrafine ferrihydrite nanoparticles, Advances in Nano Research 12 (2022) 605, https://doi.org/10.12989/anr.2022.12.6.605.
[67] Y.V. Knyazev, D.A. Balaev, S.A. Skorobogatov, D.A. Velikanov, O.A. Bayukov, S. V. Stolyar, R.N. Yaroslavtsev, R.S. Iskhakov, Spin dynamics in ensembles of ultrafine ferrihydrite nanoparticles, Phys. Rev. B 107 (2023) 115413, https://doi.org/10.1103/PhysRevB.107.115413.
[68] A.A. Bykov, S.I. Popkov, A.M. Parshin, A.A. Krasikov, Pulsed Solenoid with Nanostructured Cu–Nb Wire winding, journal of surface investigation. X-ray, Synchrotron and Neutron, Techniques 9 (N 1) (2015) 111–115, https://doi.org/10.1134/S1027451015010280.
[69] A.D. Balaev, Yu.V. Boyarshinov, M.M. Karpenko, B.P. Khrustalev, Automated magnetometer with superconducting solenoid, Instrum. Exp. Tech.(Engl. Transl.) 26 (3) [Prib. Tekh. Eksp. 3, 167 (1985)].
[70] R.D. Desautels, E. Skoropata, Y.-Y. Chen, H. Ouyang, J.W. Freeland, J. van Lierop, Increased surface spin stability in γ-Fe_2O_3 nanoparticles with a Cu shell, J. Phys. Condens. Matter 24 (2012) 146001, https://doi.org/10.1088/0953-8984/24/14/146001.
[71] E. Winkler, R.D. Zysler, D. Fiorani, Surface and magnetic interaction effects in Mn_3O_4 nanoparticles, Phys. Rev. B 70 (2004) 174406, https://doi.org/10.1103/PhysRevB.70.174406.
[72] A. Cabot, P. Alivisatos, W.F. Puntes, L. Balcells, O. Iglesias, A. Labarta, Magnetic domains and surface effects in hollow maghemite nanoparticles, Phys. Rev. B 79 (2009) 094419, https://doi.org/10.1103/PhysRevB.79.094419.
[73] J. Kurian, J.M. Mathew, A facile approach to the elucidation of magnetic parameters of $CuFe_2O_4$ nanoparticles synthesized by hydrothermal route, J. Magn. Magn. Mater. 428 (2017) 204–212, https://doi.org/10.1016/j.jmmm.2016.12.027.
[74] S.P. John, J. Mathew, Determination of ferromagnetic, superparamagnetic and paramagnetic components of magnetization and the effect of magnesium substitution on structural, magnetic and hyperfine properties of zinc ferrite nanoparticles, J. Magn. Magn. Mater. 475 (2019) 160–170, https://doi.org/10.1016/j.jmmm.2018.11.030.
[75] Xi. Chen, S. Bedanta, O. Petracic, W. Kleemann, S. Sahoo, S. Cardoso, P.P. Freitas,, Superparamagnetism versus superspin glass behavior in dilute magnetic nanoparticle systems, Phys. Rev. B 72 (2005) 214436, https://doi.org/10.1103/PhysRevB.72.214436.
[76] B.J. Sarkar, A. Bandyopadhyay, Studies of magnetic behavior of chemically synthesized interacting superparamagnetic copper ferrite nanoparticles, J. Mater. Sci. Mater. Electron. 32 (2021) 1491–1505, https://doi.org/10.1007/s10854-020-04919-x.
[77] A. Mesaros, A. Garzón, M. Nasui, R. Bortnic, B. Vasile, O. Vasile, F. Iordache, C. Leostean, L. Ciontea, J. Ros, O. Pana, Insight into synthesis and characterisation of $Ga_{0.9}Fe_{2.1}O_4$ superparamagnetic NPs for biomedical applications, Sci. Rep. 13 (2023) 18175, https://doi.org/10.1038/s41598-023-45285-y.
[78] S.S. Yakushkin, A.A. Dubrovskiy, D.A. Balaev, K.A. Shaykhutdinov, G. A. Bukhtiyarova, O.N. Martyanov, Magnetic properties of few nanometers ε-Fe_2O_3 nanoparticles supported on the silica, J. Appl. Phys. 111 (2012) 044312, https://doi.org/10.1063/1.3686647.
[79] D.A. Balaev, A.A. Krasikov, A.A. Dubrovskii, S.V. Semenov, O.A. Bayukov, S. V. Stolyar, R.S. Iskhakov, V.P. Ladygina, L.A. Ishchenko, Magnetic properties and the mechanism of formation of the uncompensated magnetic moment of antiferromagnetic ferrihydrite nanoparticles of a bacterial origin, J. Exp. Theor. Phys. 119 (3) (2014) 479–487, https://doi.org/10.1134/S1063776114080044.
[80] D.A. Balaev, S.V. Stolyar, Y.V. Knyazev, R.N. Yaroslavtsev, A.I. Pankrats, A. M. Vorotynov, A.A. Krasikov, D.A. Velikanov, O.A. Bayukov, V.P. Ladygina, R. S. Iskhakov, Results Phys. 35 (2022) 105340, https://doi.org/10.1016/j.rinp.2022.105340.
[81] Y. Wei, B. Han, X. Hu, Y. Lin, X. Wangd, X. Deng, Synthesis of Fe_3O_4 nanoparticles and their magnetic properties, Procedia Eng. 27 (2012) 632–637, https://doi.org/10.1016/j.proeng.2011.12.498.
[82] W. Wu, Q. He, H. Chen, J. Tang, L. Nie, Sonochemical synthesis, structure and magnetic properties of air-stable Fe_3O_4/Au nanoparticles, Nanotechnology 18 (2007) 145609, https://doi.org/10.1088/0957-4484/18/14/145609.
[83] M.D. Nguyen, H.-V. Tran, S. Xu T. R. Lee,, Fe_3O_4 Nanoparticles: Structures, Synthesis, Magnetic Properties, Surface Functionalization, and Emerging Applications, Appl. Sci. 11 (2021) 11301, https://doi.org/10.3390/app112311301.
[84] V. Botvin, A. Fetisova, Y. Mukhortov, D. Wagner, S. Kazantsev, M. Surmeneva, A. Kholkin, R. Surmenev, Effect of Fe3O4 Nanoparticles Modified by Citric and Oleic Acids on the Physicochemical and Magnetic Properties of Hybrid Electrospun P(VDF-TrFE) Scaffolds, Polymers 15 (2023) 3135, https://doi.org/10.3390/polym15143135.